Electronic Supplementary Material (ESI) for Sustainable Energy & Fuels.

Electronic Supporting Information

Enhancing the production of hydrogen peroxide from electrocatalytic oxygen reduction reaction by tailoring the electronic states of single-walled carbon nanotubes: a synergistic effect from interior filling and exterior oxidation

Rongtao Hu[ac], Fenfa Yao[b], Chuxin Wu[a], Chuanhong Jin[b] and Lunhui Guan*[a]

a.CAS Key Laboratory of Design and Assembly of Functional Nanostructures, and Fujian Key Laboratory of Nanomaterials, Fujian Institute of Research on the Structure of Matter, Chinese Academy of Sciences, Fuzhou, Fujian 350002, China

b.State Key Laboratory of Silicon Materials, School of Materials Science and Engineering, Zhejiang University, Hangzhou, Zhejiang 310027, China

c.University of Chinese Academy of Sciences, Beijing 100049, China

* Corresponding Author. Tel: +86-591-63173550. E-mail: guanlh@fjirsm.ac.cn

Table S1 The record on mass change of filling process.

Initial substance and mass (mg)		Final substance and mass (mg)	△m%
SWCNT	10.07	HPMO@SWCNT 16.65	65.34%
	9.89	16.03	62.08%
	9.97	16.21	62.59%
	9.80	15.22	55.31%
	9.80	16.36	66.94%
	9.78	17.10	74.85%

Annotation: △m% = (Final mass/Intial mass - 1) × 100%

Table S2 The contrasts in onset potential and Tafel slope.

Electrocatalyst	Onset potential (V)	Tafel slope (mV/dec)
SWCNT	0.722	47.89
HPMO@SWCNT	0.742	48.19
O-HPMO@SWCNT	0.792	34.57
O-SWCNT	0.782	34.84

Table S3 ORR Performance of several reported electrocatalysts.

Electrocatalyst	Selectivity (%)	Steady ring current in stability test (mA)	Reference
O-HPMO@SWCNT	80	0.35	This work
Nitrogen-doped graphrene oxide	82	0.20	ACS Catal. 2019, 9, 2, 1283-1288
Oxidized ordered mesoporous graphitic carbon	90	0.50	Angew. Chem. Int. Ed. 2019, 58, 1100-1105
h-BN domains within graphitic lattice	80	0.25	J. Am. Chem. Soc. 2018, 140, 7851-7859
Oxidized MWCNTs	90	0.43	Nat. Catal. 2018, 1(2), 156-162

Table S4 The summary of ring current at 0.40 V Vs. RHE and atomic percentage of oxygen estimated by XPS survey spectra of samples.

Electrocatalyst	Atomic percentage of oxygen (%)	Ring current @ 0.40 V Vs. RHE (mA)
SWCNT	3.14	0.19
HPMO@SWCNT	16.77	0.23
O-HPMO@SWCNT	23.95	0.34
O-SWCNT	32.69	0.27

Table S5 The summary of ring current at 0.40 V Vs. RHE and value of I_D/I_G in all the samples.

Electrocatalyst	I_D/I_G	Ring current @ 0.40 V Vs. RHE (mA)
SWCNT	0.07	0.19
HPMO@SWCNT	0.05	0.23
O-HPMO@SWCNT	0.78	0.34
O-SWCNT	0.96	0.27

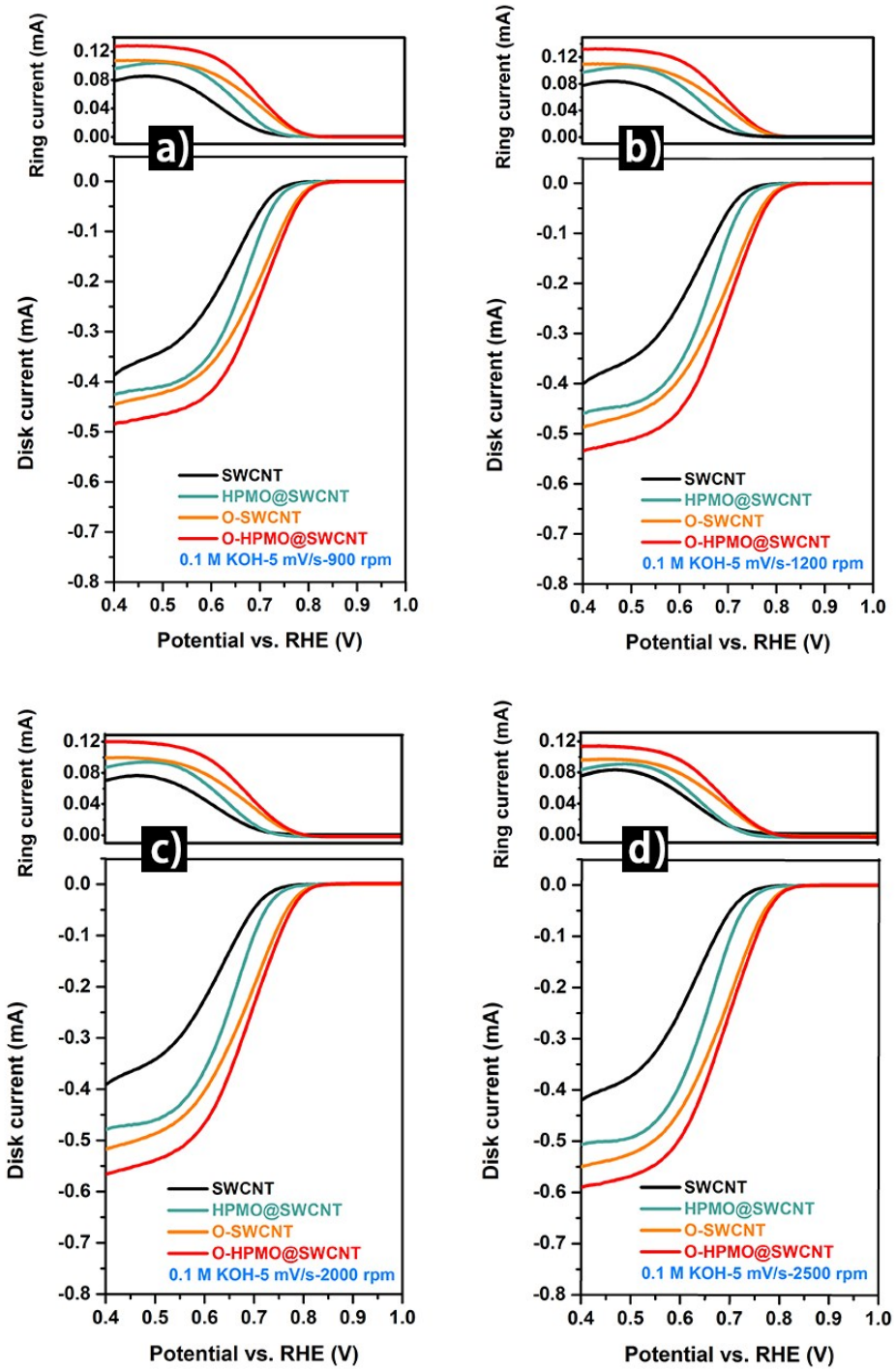

Fig. S1 Linear Sweep Voltammetry (LSV) curves of the samples. All the LSV curves were recorded on Rotating Ring Disk Electrode (RRDE, Pt ring (0.186 cm^{-2}) and glassy carbon disk (0.247 cm^{-2})) in 0.1 M KOH with rotation rate of 900 (a), 1200 (b), 2000 (c), 2500 (d) rpm and potential scan rate of 5 mV/s. Upper lines represent measured ring current and lower lines mean measured disk current.

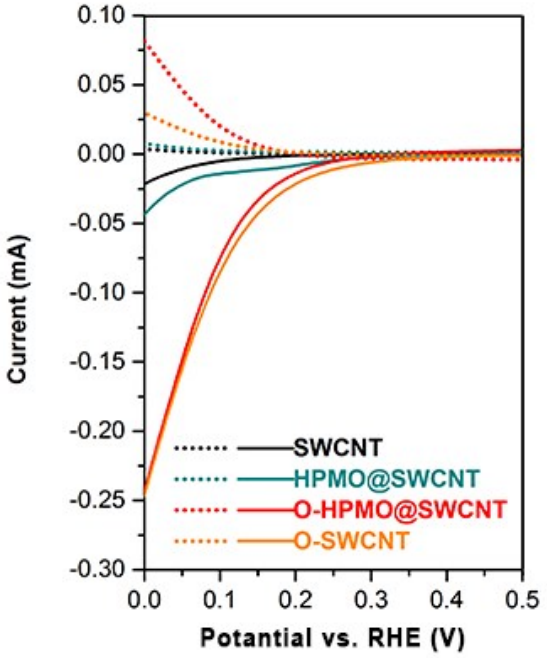

Fig. S2 Linear Sweep Voltammetry (LSV) curves of the samples. All the LSV curves were recorded on Rotating Ring Disk Electrode (RRDE, Pt ring (0.186 cm^{-2}) and glassy carbon disk (0.247 cm^{-2})) in 0.1 M $HClO_4$ with rotation rate of 1600 rpm and potential scan rate of 5 mV/s. Dashed lines represent measured ring current divided by collection efficiency *N*c and solid lines mean measured disk current.

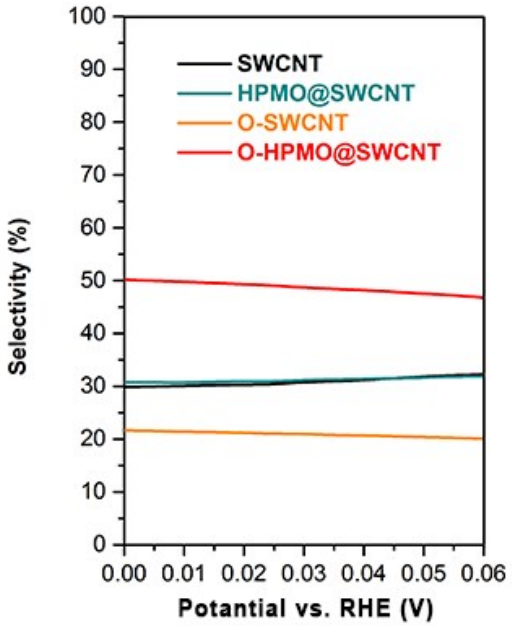

Fig. S3 Calculated selectivity towards H_2O_2 at various potentials in 0.1 M $HClO_4$ of the samples.

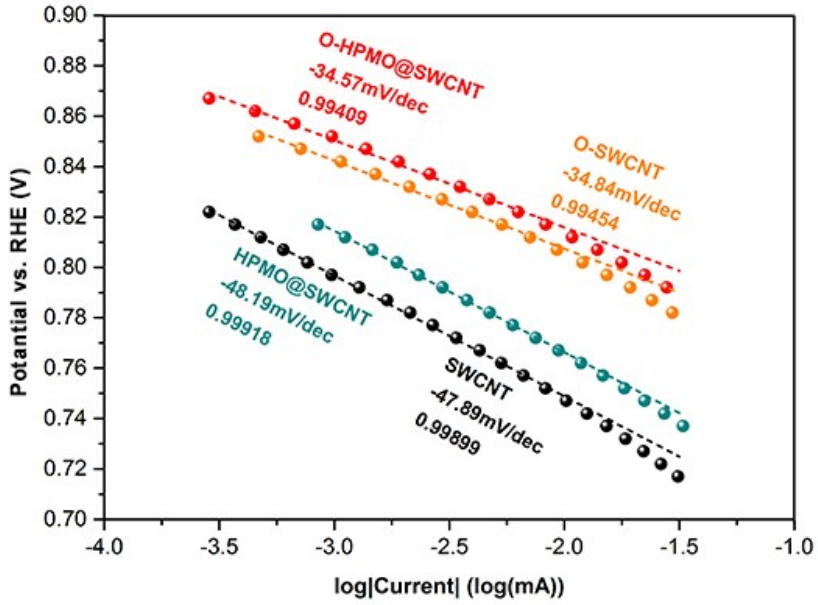

Fig. S4 The calculation on Tafel slope of all the samples from LSV curves recorded in 0.1 M KOH.

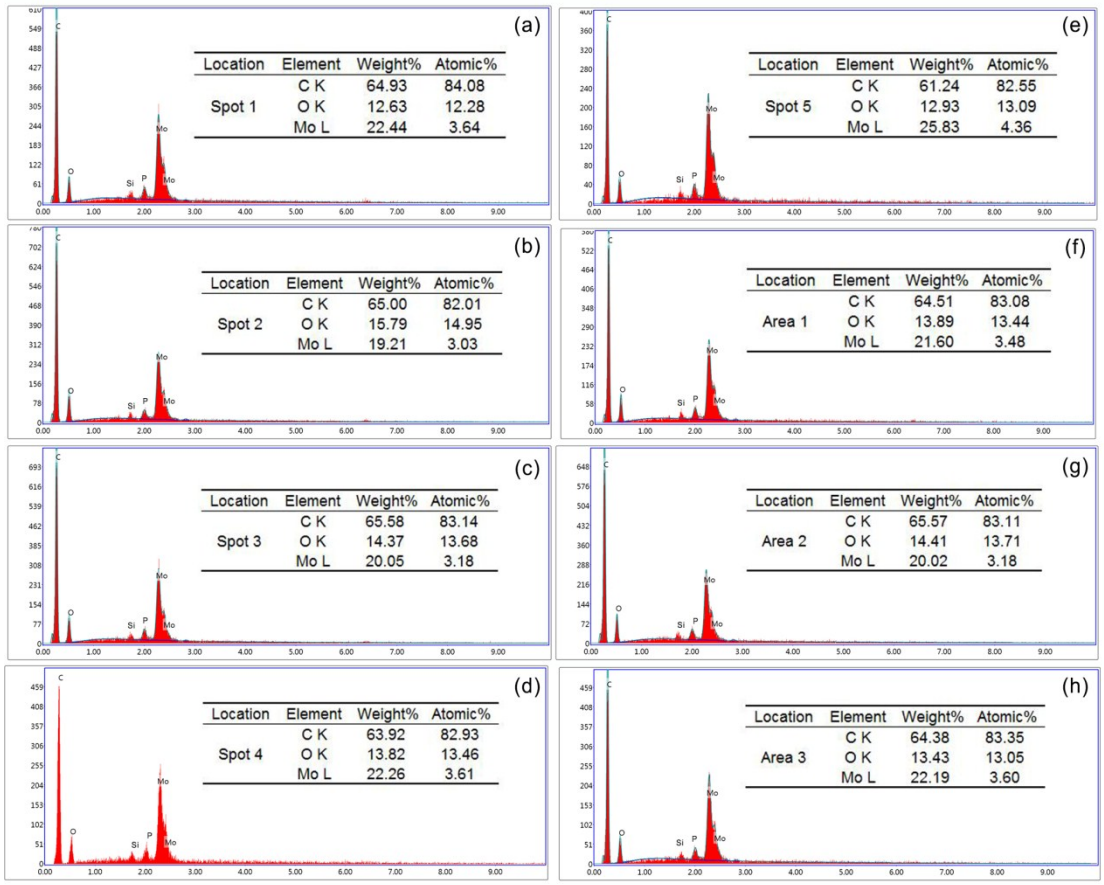

Fig. S5 The original data and spectra on EDS of HPMO@SWCNT.

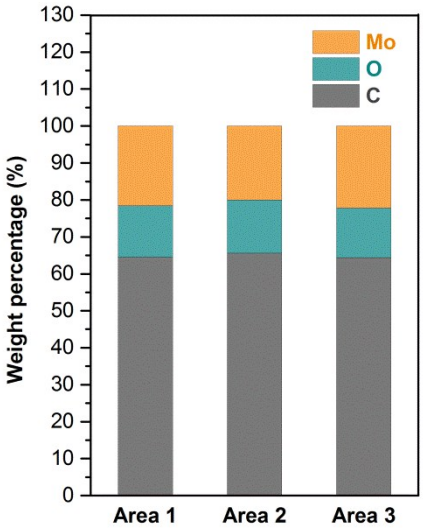

Fig. S6 The bar diagram on EDS of HPMO@SWCNT.

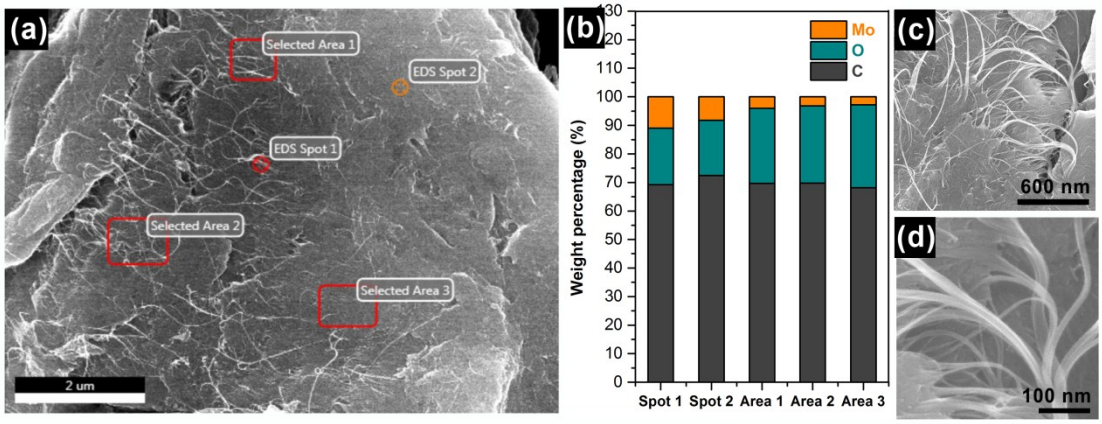

Fig. S7 Microscale analysis on components and geometrical structure of O-HPMO@SWCNT. SEM image of HPMO@SWCNT with scale bar of 2 μm (a). Elements distribution in O-HPMO@SWCNT characterized by EDS (b). SEM images of O-HPMO@SWCNT with scale bar of 600 nm (c) and 100 nm (d).

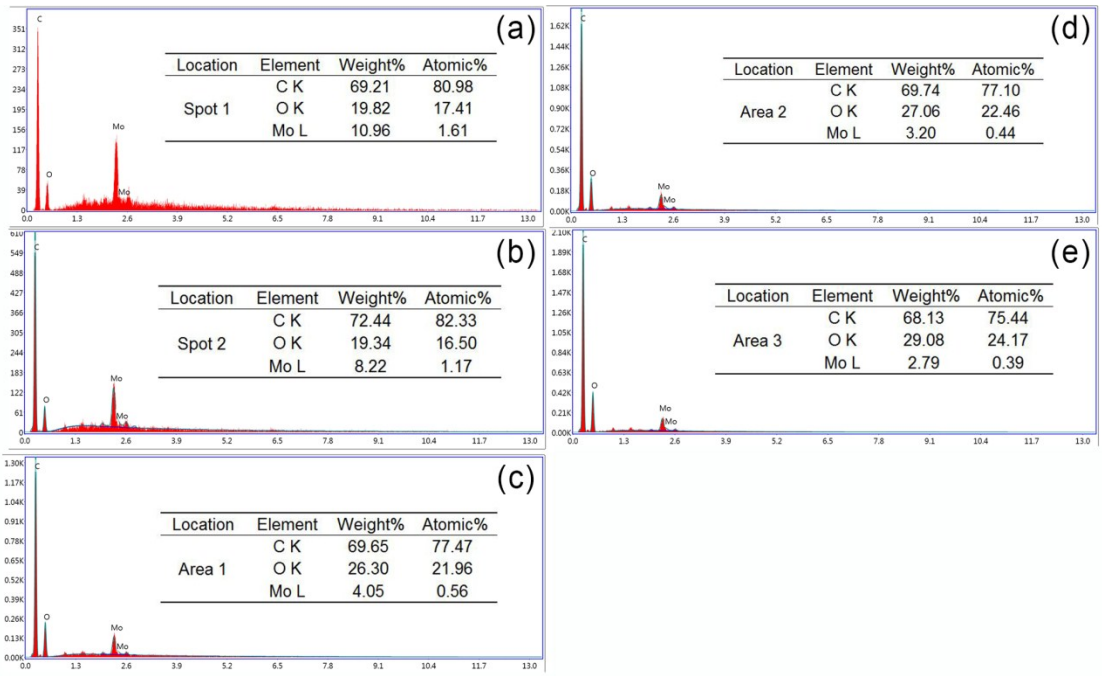

Fig. S8 The original data and spectra on EDS of O-HPMO@SWCNT.

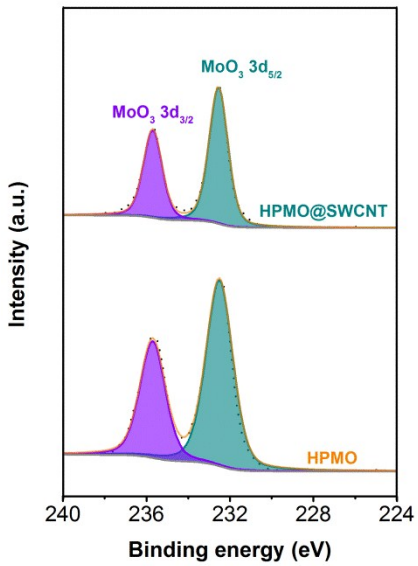

Fig. S9 The XPS detailed Mo 3d spectra of HPMO@SWCNT and HPMO.

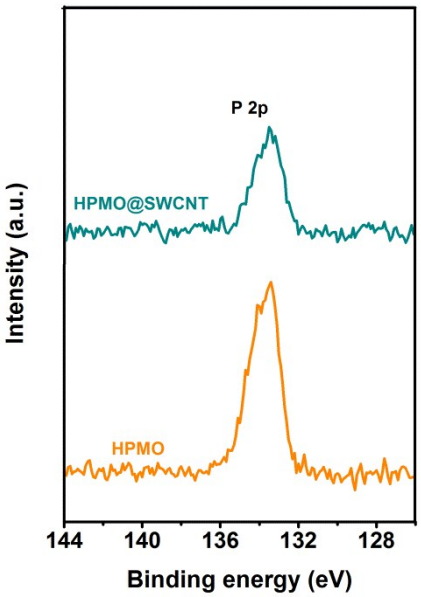

Fig. S10 The XPS detailed P 2p spectra of HPMO@SWCNT and HPMO.

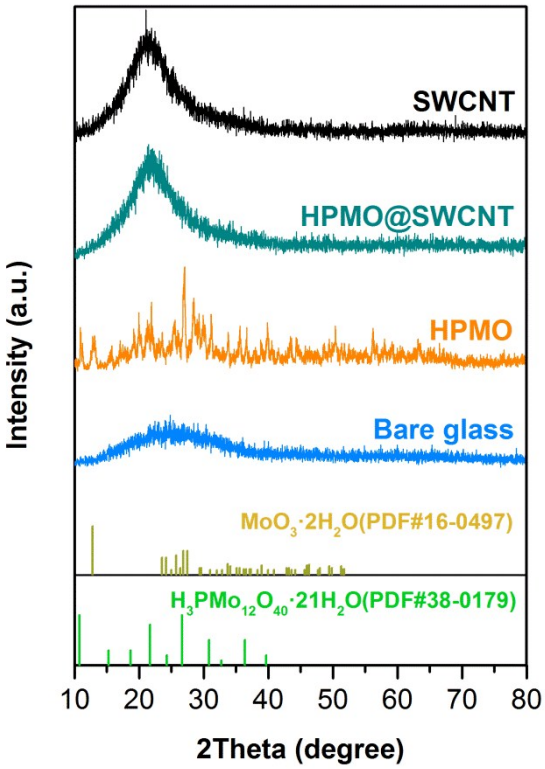

Fig. S11 The Powder X-ray diffraction patterns of SWCNT, HPMO@SWCNT and HPMO.

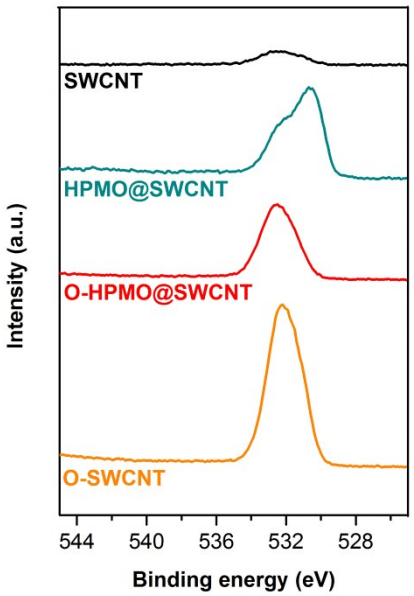

Fig. S12 The XPS detailed O 1s spectra of all the samples.

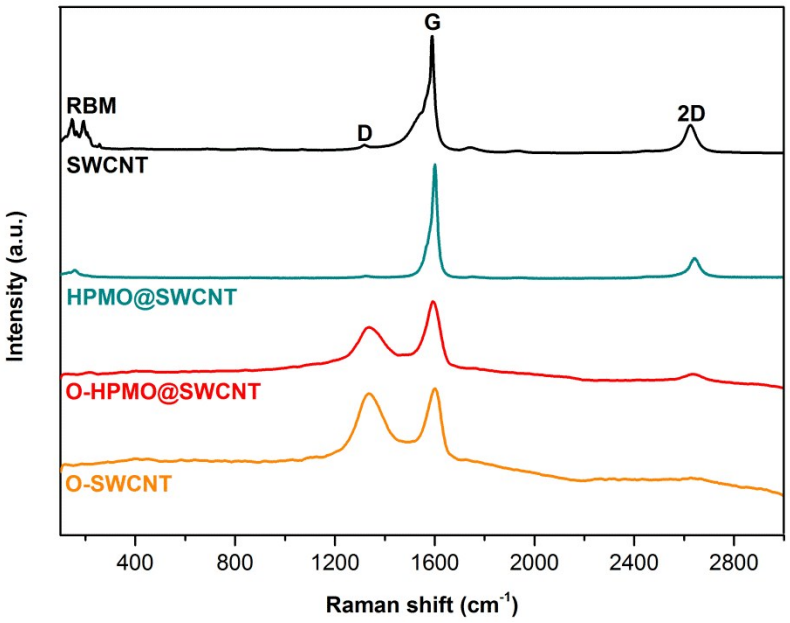

Fig. S13 The original Raman spectra of all the samples.

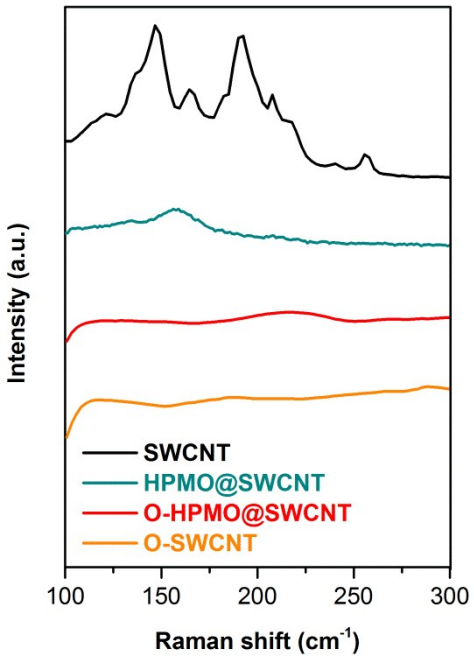

Fig. S14 Raman spectra of the samples at region from 100 cm^{-1} to 300 cm^{-1}.

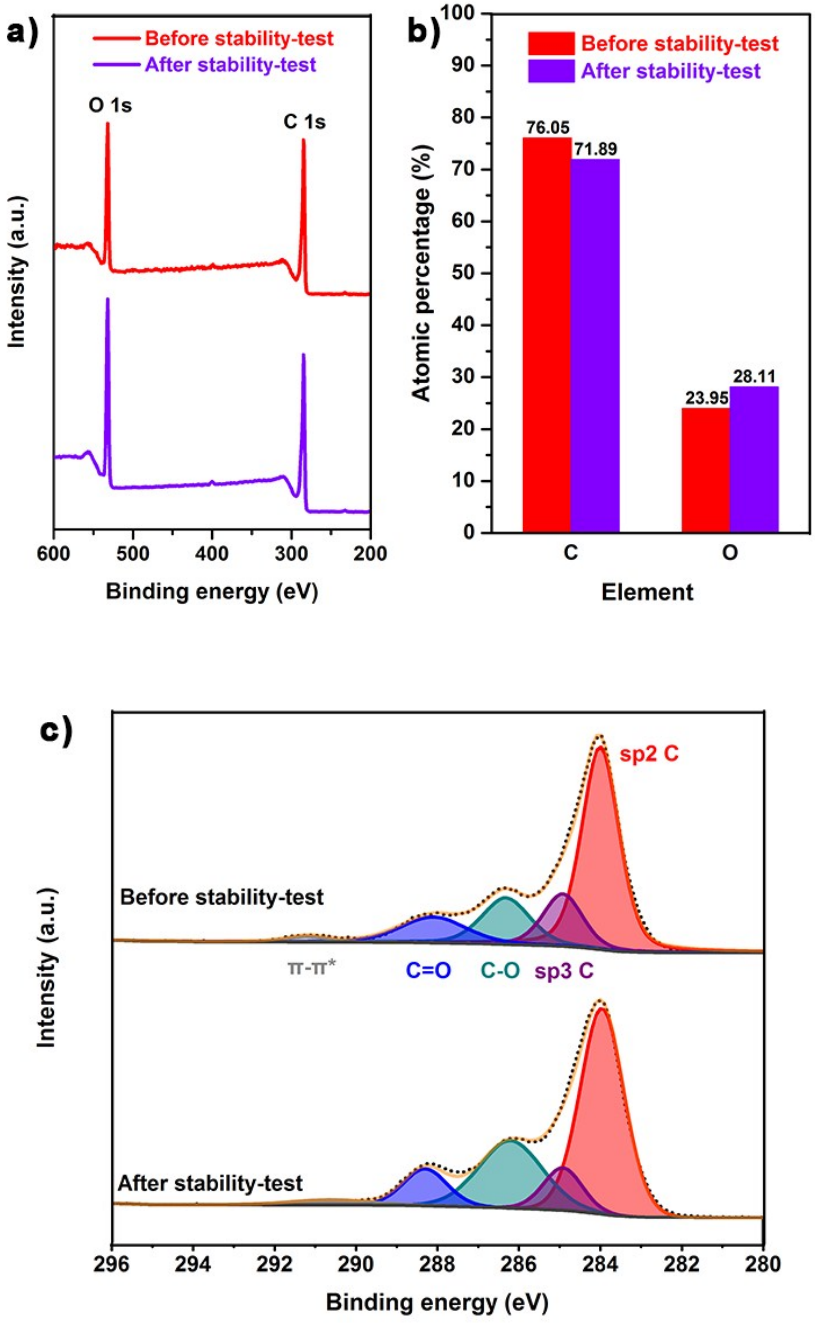

Fig. S15 XPS of O-HPMO@SWCNT before and after stability-test. a) Survey scan spectra. b) Atomic percentage of carbon and oxygen derived from survey scan spectra. c) Detailed C 1s spectra.

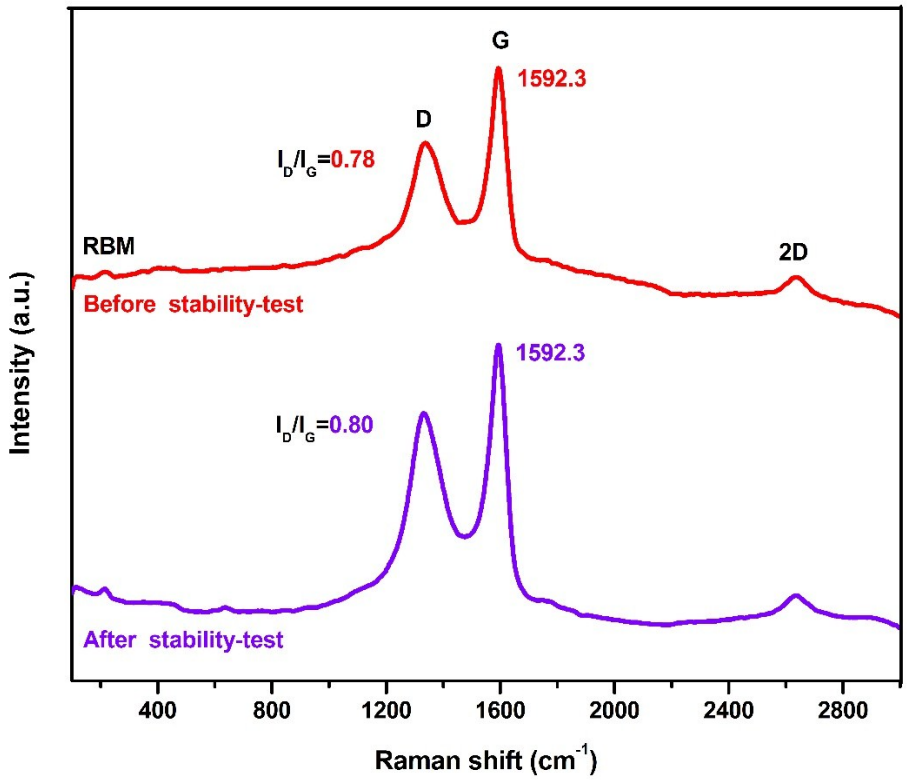

Fig. S16 Raman spectroscopy of O-HPMO@SWCNT before and after stability-test.